Supporting Information

Oxygen Defect-induced Localized Surface Plasmon Resonance in WO3-x Quantum Dot/Silver Nanowire Interface: Photocatalysis and SERS

Wei Wei,‡[a] Yongji Yao,‡[a] Qi Zhao,[a] Zhilong Xu[a], Qinfan Wang[a], Zongtao Zhang[b] and Yanfeng Gao*[a]

[a]*School of Materials Science and Engineering, Shanghai University, Shanghai 200444, People's Republic of China. E-mail: yfgao@shu.edu.cn*
[b]*School of Materials Science and Engineering, Zhengzhou University, Zhengzhou, Henan, 450001, People's Republic of China.*
‡Contributed equally to this work.

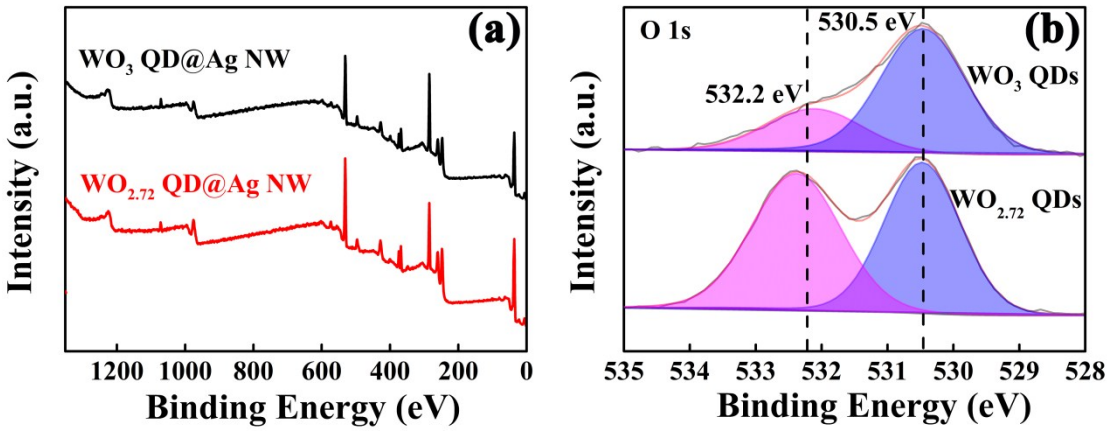

Figure S1. XPS spectra of $WO_{2.72}$ QD@Ag NW and WO_3 QD@Ag NW: (a) survey spectra and (b) high-resolution O 1s spectra.

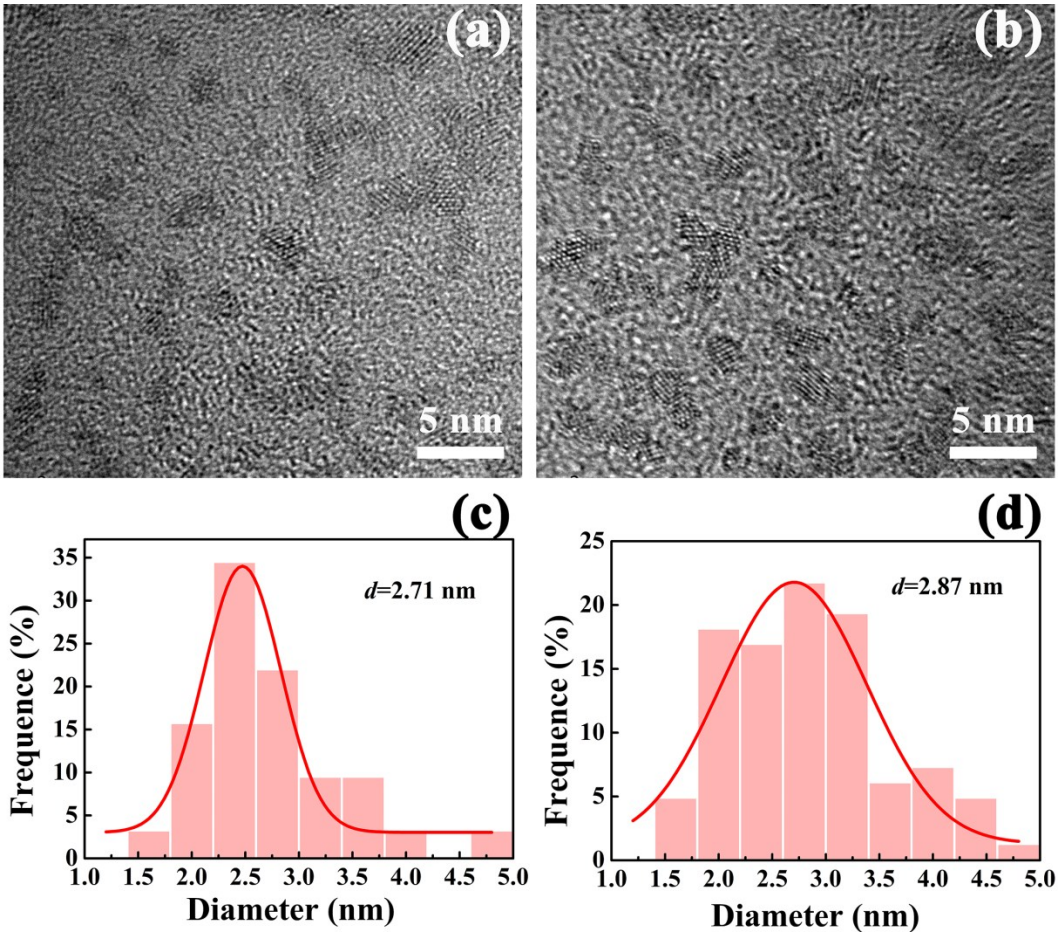

Figure S2. TEM images of (a) WO_3 QDs and (b) $WO_{2.72}$ QDs. Diameter distributions of (c) WO_3 QDs and (d) $WO_{2.72}$ QDs.

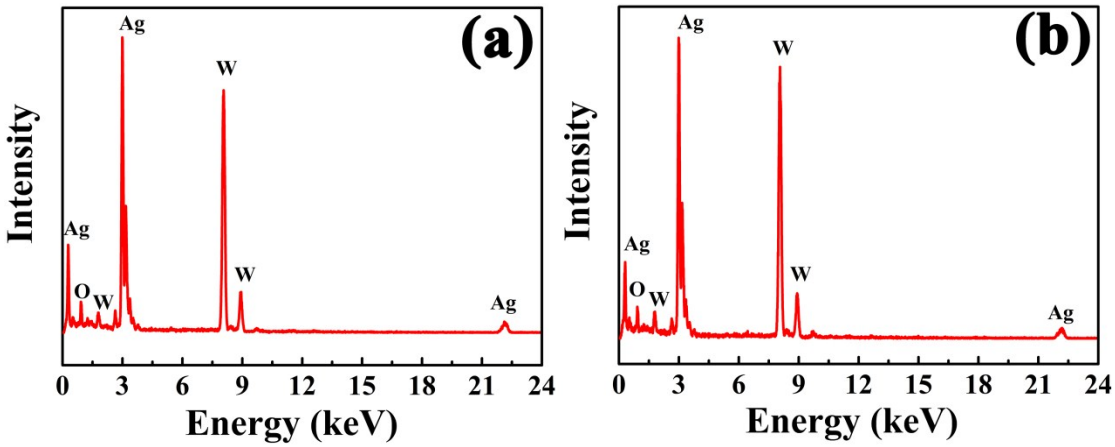

Figure S3. EDS spectra of (a) WO_3 QD@Ag NW hybrids in Figure 2a, and (b) $WO_{2.72}$ QD@Ag NW hybrids in Figure 2b.

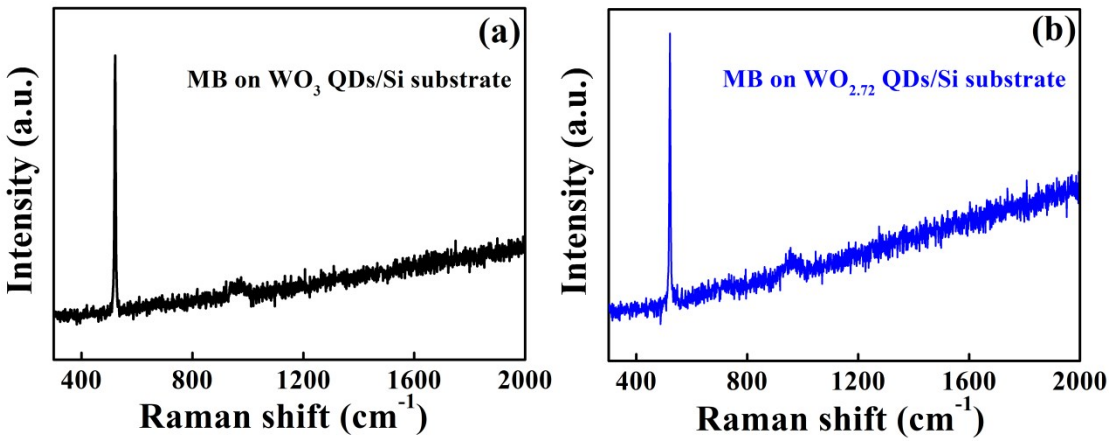

Figure S4. Raman spectra of (a) MB on WO_3 QDs/Si substrate and (b) MB on $WO_{2.72}$ QDs/Si substrate. Herein, ten microlitres of Methylene blue (MB) with a fixed concentration (1×10^{-6} M) was added dropwise onto the surface of the as-prepared WO_{3-x} QD@Ag NW substrate and then measured at an excitation wavelength of 633 nm.

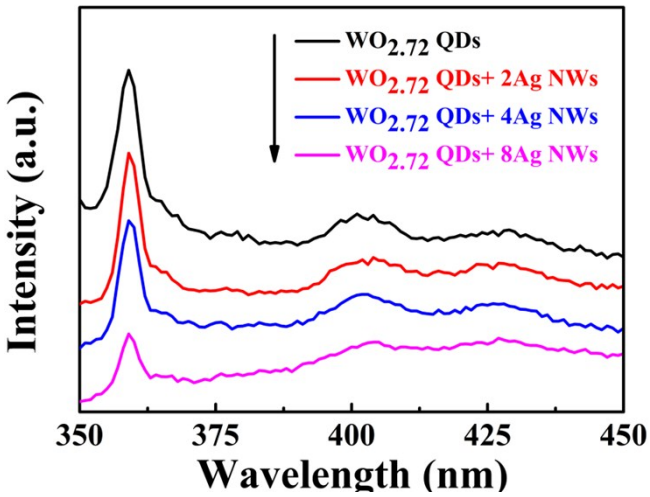

Figure S5. PL spectra of $WO_{2.72}$ QDs and $WO_{2.72}$ QD@Ag NW with an excitation light of 325 nm.

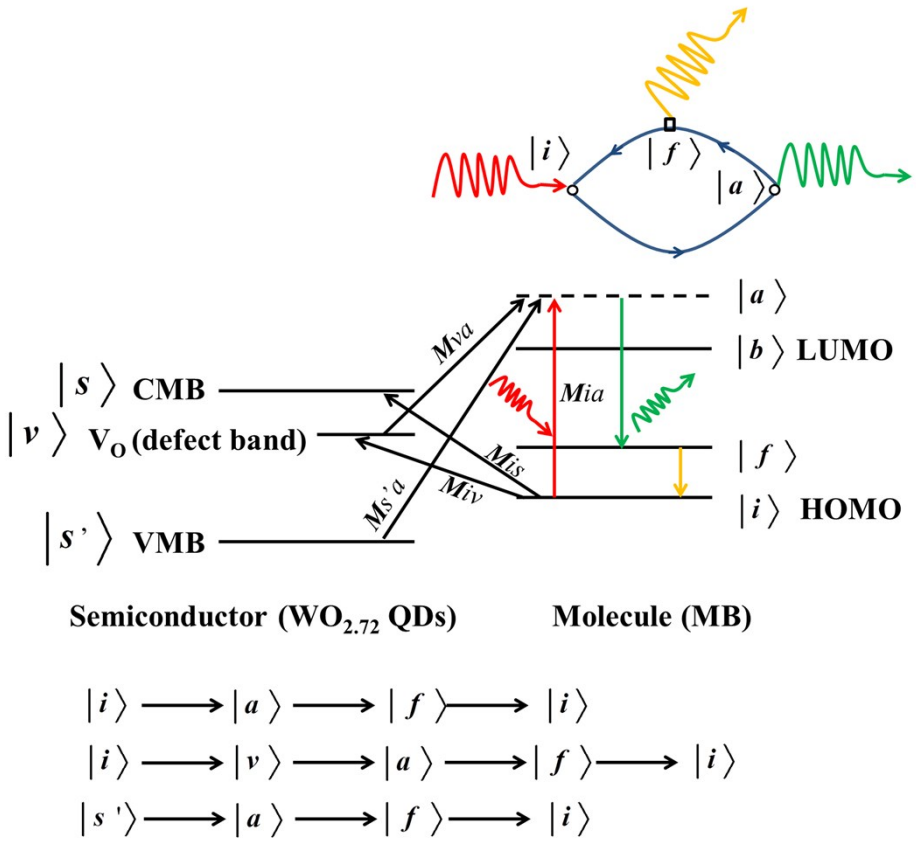

Figure S6. The scheme of a Raman scattering process described by Feynman figure, and the photo-induced charge transfer of semiconductor-to-molecule and molecule-to-semiconductor for a defect-rich semiconductor.

A Raman scattering process of MB molecule can be illustrated by the Feynman figure (Figure S5). An ordinary Raman scattering process includes the following aspects as the quantum theory: (1) the photon-electron interaction in ground state (LOMO), electrons gain energy and jump to excited state; (2) the electrons transition from excited state to final state, resulting in the generation of photons (scattering light); (3) the coupling between phonons (or vibrational mode) and electrons, these electrons fall back to the ground state. According to the Fermi's golden rule, the Raman scattering probability (P_s) is proportional to the one-to-many transition probability per unit of time from the initial state $|i\rangle$ to a set of final states $|f\rangle$. The Raman scattering intensity (I_s) as given by the Golden Rule will be:[1]

$$I_s \propto P_s = \frac{2\pi}{\mathrm{h}}\left|\frac{\langle i|H_{\text{e-ph}}|f\rangle\langle f|H_{\text{e-r}}(\omega_s)|a\rangle\langle a|H_{\text{e-r}}(\omega_i)|i\rangle}{\left[\left(\mathrm{h}\omega_i-(E_a-E_i)\right]\left[\mathrm{h}\omega_i-\mathrm{h}\omega_0-\left(E_f-E_i\right)\right]}\right|^2 \delta(\mathrm{h}\omega_i-\mathrm{h}\omega_s-\mathrm{h}\omega_0) \quad \text{(S1)}$$

where $|i\rangle$ and $|f\rangle$ represent the initial state and final state of electrons, respectively. $|a\rangle$ represent the excited state. $H_{\text{e-r}}$ and $H_{\text{e-ph}}$ are the Hamiltonian matrix of radiation light and electron-phonon coupling. E_a and E_i is the energy of excited state $|a\rangle$ and ground state $|i\rangle$. $\hbar\omega_i$, $\hbar\omega_s$ and $\hbar\omega_0$ is the energy of the incident photon, scattered photon and emitted phonon respectively. However, in the defect-rich semiconductor-molecule system, the contribution of photo-induced charge transfer (PICT) to Raman scattering must be taken into consideration.[2] The rich oxygen vacancies in $WO_{2.72}$ QDs can introduce new electronic states (Figure S9), which benefit to the Raman scattering. Here, we use $|s'\rangle$ to denote electronic state the top of the valence band, and $|v\rangle$ represent the oxygen defect state lying in the forbidden band. These electronic states in lattice or surface provide two new pathways for electron transfer: (1) $|i\rangle\rightarrow|v\rangle\rightarrow|a\rangle\rightarrow|f\rangle\rightarrow|i\rangle$; (2) $|s'\rangle\rightarrow|a\rangle\rightarrow|f\rangle\rightarrow|i\rangle$.[3] With a similar approach, we write:

$$I_s \propto P_s = \frac{2\pi}{\mathrm{h}}\left|\mathrm{A}+\mathrm{B}+\mathrm{C}\right|^2 \delta(\mathrm{h}\omega_i-\mathrm{h}\omega_s-\mathrm{h}\omega_0) \quad \text{(S2)}$$

$$\mathrm{A} = \frac{\langle i|H_{\text{e-ph}}|f\rangle\langle f|H_{\text{e-r}}(\omega_s)|a\rangle\langle a|H_{\text{e-r}}(\omega_i)|i\rangle}{\left[\left(\mathrm{h}\omega_i-(E_a-E_i)\right]\left[\mathrm{h}\omega_i-\mathrm{h}\omega_0-\left(E_f-E_i\right)\right]} \quad \text{(S3)}$$

$$\mathrm{B} = \frac{\langle i|H_{\text{e-ph}}|f\rangle\langle f|H_{\text{e-r}}(\mathrm{h}\omega_s)|a\rangle\langle a|H_{\text{e-r}}(\mathrm{h}\omega_i)|v\rangle\langle v|H_{\text{e-r}}(\mathrm{h}\omega_i)|i\rangle}{\left[\left(\mathrm{h}\omega_i-(E_a-E_i)\right]\left[\mathrm{h}\omega_i-\mathrm{h}\omega_0-\left(E_f-E_i\right)\right]} \quad \text{(S4)}$$

$$\mathrm{C} = \frac{\langle i|H_{\text{e-ph}}|f\rangle\langle f|H_{\text{e-r}}(\mathrm{h}\omega_s)|a\rangle\langle a|H_{\text{e-r}}(\mathrm{h}\omega_i)|s'\rangle}{\left[\left(\mathrm{h}\omega_i-(E_a-E_{s'})\right]\left[\mathrm{h}\omega_i-\mathrm{h}\omega_0-\left(E_f-E_{s'}\right)\right]} \quad \text{(S5)}$$

here A represents the contribution of adsorbed molecular resonance, which is independent of the defect states in the semiconductor. B represents the contribution of

PICT, which is resulted from defect states in the semiconductor-molecular system, especially in the irradiated $WO_{2.72}$ QDs, more electrons occupied the oxygen defect state helped to increase the transition probability of photon-generated electrons. C represents the contribution of PICT from valance state to an excited state of the molecule.

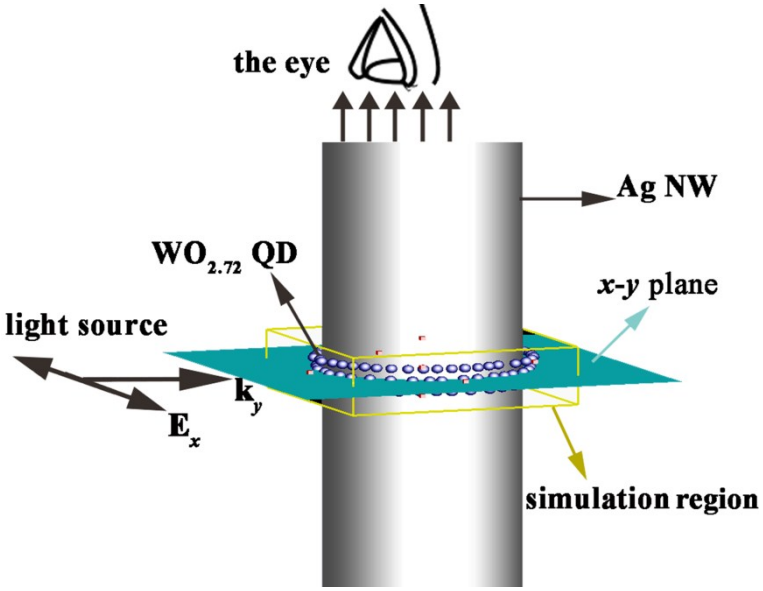

Figure S7. Schematic diagram of FDTD simulation for $WO_{2.72}$ QD@Ag NW structure. The spatial electric field distribution maps in the *x-y* plane were extracted from this calculations. The diameter of $WO_{2.72}$ QD and Ag NW are 2.8 nm and 50 nm, respectively.

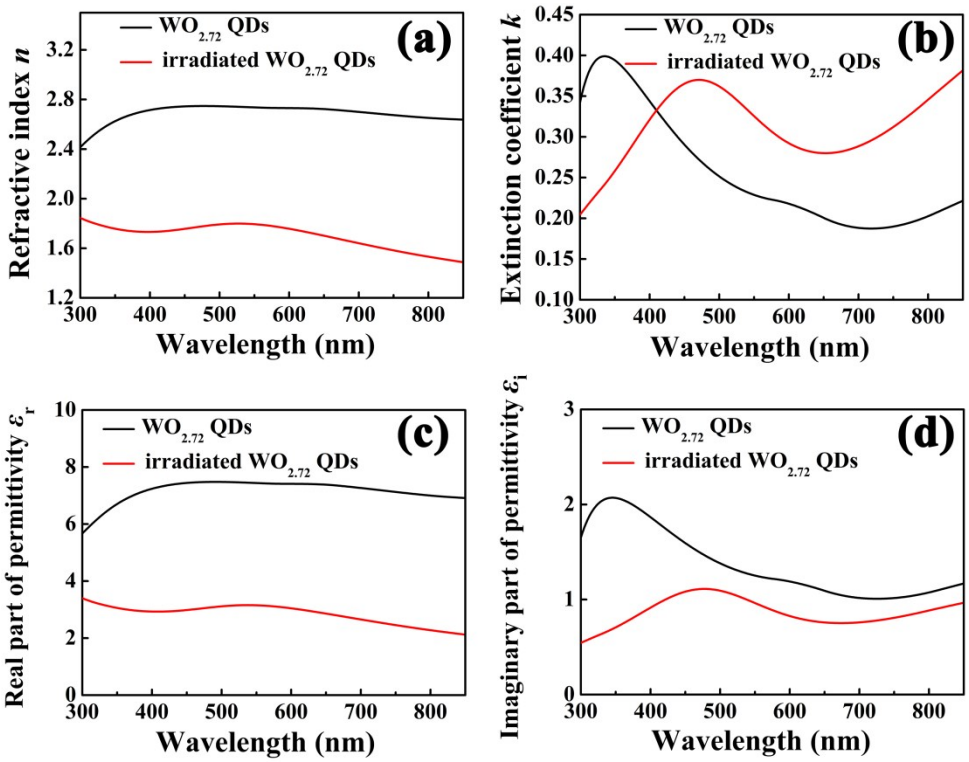

Figure S8. (a) Refractive index n, (b) extinction coefficient k, (c) real part of permittivity ε_r and (d) imaginary part of permittivity ε_i of $WO_{2.72}$ QDs and irradiated $WO_{2.72}$ QDs.

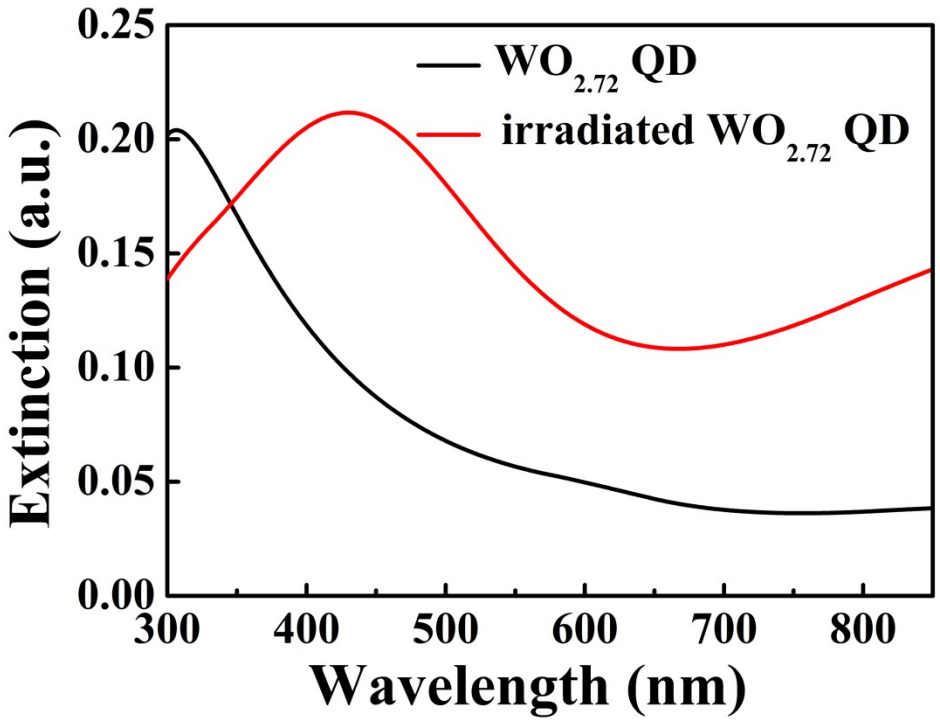

Figure S9. The simulated extinction spectrum of a $WO_{2.72}$ QD of radius a=1.4 nm in air. This result has same trends as the measured UV-vis absorption spectra of $WO_{2.72}$ QDs dispersion (in ethanol).

In this simulation, we consider a spherical $WO_{2.72}$ QD of radius a=1.4 nm that is irradiated by x-polarized light of wavelength λ (Figure S6). The extinction spectrum of the single $WO_{2.72}$ QD can be calculated as follow:[4,5]

$$E(\lambda) = \frac{24\pi^2 a^3 \varepsilon_{out}^{3/2}}{\lambda \ln(10)} \left[\frac{\varepsilon_i(\lambda)}{\left(\varepsilon_r(\lambda) + \chi\varepsilon_{out}\right)^2 + \varepsilon_i(\lambda)} \right] \quad \text{(S6)}$$

here, ε_r and ε_i are the real and imaginary components of the dielectric constant (in Figure S7), respectively. ε_{out} is the external dielectric constant (ε_{out}=1 for air), λ is the wavelength of the incident x-polarized light. The value of factor χ is 2 for the case of a sphere.

References

1. P. Y. Yu and M. Cardona, *Fundamentals of Semiconductors: Physics and Materials Properties*, Springer, Heidelberg, 2005.
2. S. Cong, Y. Yuan, Z. Chen, J. Hou, M. Yang, Y. Su, Y. Zhang, L. Li, Q. Li, F. Geng, Z. Zhao, *Nat. Commun.*, 2015**, 6**, 7800.
3. J. R. Lombardi, R. L. Birke, *J. Phys. Chem. C*, 2014, **118**, 11120-11130.
4. K. A. Willets, R. P. Van Duyne, *Annu. Rev. Phys. Chem.*, 2007, **58**, 267-297.
5. C. F. Bohren, D. R. Huffman, *Absorption and Scattering of Light by Small Particles*, Wiley, New York, 1983.